Type IX Collagen Interacts with Fibronectin Providing an Important Molecular Bridge in Articular Cartilage*

Philippa Parsons[‡]**, Sophie J. Gilbert**[§]**, Anne Vaughan-Thomas**[¶†]**, David A. Sorrell**[∥]**, Rebecca Notman**[§]**, Mark Bishop**[§]**, Anthony J. Hayes**[§]**, Deborah J. Mason**[§]**, and Victor C. Duance**[§1]

From the [‡]*Research Centre, Smith & Nephew, York Science Park, Heslington, York YO10 5DF, the* [§]*Pathophysiology and Repair Division, School of Biosciences, Cardiff University, Museum Avenue, Cardiff CF10 3AX, the* [¶]*Faculty of Veterinary Science, University of Liverpool, Veterinary Sciences Building, Liverpool L69 7ZJ, and the* [∥]*Horizon Discovery Services, 260 Cambridge Science Park, Milton Road, Cambridge CB4 0WE, United Kingdom*

Type IX collagen is covalently bound to the surface of type II collagen fibrils within the cartilage extracellular matrix. The N-terminal, globular noncollagenous domain (NC4) of the $\alpha1$(IX) chain protrudes away from the surface of the fibrils into the surrounding matrix and is available for molecular interactions. To define these interactions, we used the NC4 domain in a yeast two-hybrid screen of a human chondrocyte cDNA library. 73% of the interacting clones encoded fibronectin. The interaction was confirmed using *in vitro* immunoprecipitation and was further characterized by surface plasmon resonance. Using whole and pepsin-derived preparations of type IX collagen, the interaction was shown to be specific for the NC4 domain with no interaction with the triple helical collagenous domains. The interaction was shown to be of high affinity with nanomolar K_d values. Analysis of the fibronectin-interacting clones indicates that the constant domain is the likely site of interaction. Type IX collagen and fibronectin were shown to co-localize in cartilage. This novel interaction between the NC4 domain of type IX collagen and fibronectin may represent an *in vivo* interaction in cartilage that could contribute to the matrix integrity of the tissue.

The organization and interactions of the extracellular matrix (ECM)[2] of articular cartilage provide its unique mechanical properties. A network composed of stable collagen fibrils confers tensile strength to articular cartilage to resist the repeated loading as occurs *in vivo*. The principal components of this network are collagen types II, IX, and XI, forming heterotypic fibrils, in which type IX collagen is covalently cross-linked to the surface of type II collagen in a D-periodic arrangement along the fibrils (1–4). The concept of heterotypic fibrils is well established, although the functional roles of type IX collagen within articular cartilage remain unclear.

A member of the fibril-associated collagens with an interrupted triple helix (FACIT) family of collagens, type IX is a heterotrimer of three genetically distinct polypeptide chains, $\alpha1$(IX), $\alpha2$(IX), and $\alpha3$(IX), stabilized by interchain disulfide bonds. The complete molecule consists of three triple helical domains (COL1–3) and four noncollagenous domains (NC1–4) (for reviews see Refs. 5, 6). Rotary shadowing electron microscopy has revealed a "kink" in the NC3 domain. This elevates the COL3 and the N-terminal globular NC4 domains of the $\alpha1$(IX) chain away from the heterotypic fibril surface projecting it into the surrounding matrix (7, 8). This position makes the COL3 and NC4 domains ideal candidates for interactions with other matrix molecules. *In vitro* studies substantiate this hypothesis.

The COL3 domain has been shown to interact strongly with the I domain of integrins using a novel binding site possibly involving amino acids from more than one chain (8). Thus, type IX collagen is implicated in cell adhesion to the type II/XI/IX collagen macromolecular alloy. The $\alpha1$(IX) NC4 domain also interacts with thrombospondin 5 (TSP5), also known as cartilage oligomeric protein (COMP) (9), which, as a pentamer, can participate in multiple interactions, including an interaction with matrilin-3 (10). Type IX collagen can also interact with matrilin-3 directly through a binding site in the COL3 domain (11) implicating matrilin-3 as an interface component, linking macromolecular networks. Furthermore, the basic NC4 domain of the $\alpha1$(IX) chain can interact with heparin (12) and also the N-terminal tyrosine sulfate-rich domain of fibromodulin (13). As a consequence of all of the interactions in which type IX collagen can participate, it is not surprising that its perceived function is to stabilize and organize the fibrillar collagen network in cartilage.

Type IX collagen exists as a long or a short form depending on the presence or absence of the NC4 domain that is regulated by an alternative promoter in intron 6 of the *COL9A1* gene (14). The existence of this alternative promoter in the *COL9A1* gene is indicative of a specific functional role for the NC4 domain. The specific expression of the NC4 domain in cartilage (14) and its pericellular localization (15) has identified a potential role in remodeling the cartilage matrix. In addition, loss of type IX collagen in aging articular cartilage may result in a weaker matrix that is more susceptible to degradation (16, 17). More recently, analysis of human articular cartilage has determined that both the C terminus of type IX collagen and the NC4

domain are lost from the territorial and interterritorial matrices after maturation but are maintained in the pericellular matrix in articular cartilage throughout life (1, 18).

Studies on transgenic mice have supported the hypothesis that NC4 domain interactions play an important role in articular cartilage matrix integrity. Several transgenic mice expressing abnormal type IX collagen have been produced, all of which exhibit a form of degenerative joint disease similar to osteoarthritis (OA) (19–21). Homozygous α1(IX) knock-out mice are viable but develop a severe degenerative joint disease that is similar to OA, as early as 4 months (20). Transgenic mice expressing a truncated α1(IX) chain also develop degenerative joint disease with the severity of disease correlating with the level of transgene expression (19). Importantly, overexpression of the NC4 domain alone also caused a degenerative joint disease phenotype, shown to be significant in mice between 11 and 21 months old (21), indicating a specific role for NC4 interactions in maintaining cartilage matrix integrity.

Col9a1 gene knockouts in combination with various thrombospondins result in disruption of the growth plate (22, 23), and *Col9a1/TSP5* double knock-out mice are particularly prone to exercise-induced articular cartilage degradation (23). These studies show that the absence of type IX collagen and in some instances specific disruption of the NC4 domain predisposes articular cartilage to OA-like degradation, indicating that the NC4 domain and type IX are important for long term tissue stability and cartilage matrix integrity.

Human diseases associated with mutations in the genes encoding type IX collagen also provide evidence for its role in articular cartilage matrix stability. Type IX collagen mutations have been linked with the autosomal dominant disease, multiple epiphyseal dysplasia, characterized by short stature and severe joint pain caused by early onset, sometimes pre-adolescent, OA. Multiple epiphyseal dysplasia causing mutations identified in all three type IX collagen genes are located within the N terminus of the COL3 domain of the molecule. Mutations in *COL9A2* and *COL9A3* genes result in skipping of exon 3, leading to the in-frame deletion of 12 amino acids within the equivalent regions of the COL3 domain of the α2(IX) and α3(IX) chains (for review see Ref. 24). A single mutation in the *COL9A1* gene that is linked to an unclassified phenotype of multiple epiphyseal dysplasia has been identified that gives rise to an in-frame deletion, also at the N-terminal end of the COL3 domain, of either 21, 25, or 49 amino acids (25). Such deletions within any one of the three chains encoding the COL3 domain of type IX collagen may significantly alter the tertiary structure of the molecule. This may result in a shift in the spatial arrangement of the NC4 domain, impairment of NC4 matrix interactions, and consequently the characteristic cartilage degradation observed in this disease.

To elucidate the protein-protein interactions of the NC4 domain of type IX collagen in articular cartilage, we used the NC4 domain as "bait" in a yeast two-hybrid screen of a human chondrocyte cDNA library. 73% of interacting clones were found to encode cellular fibronectin (FN). Molecular analysis of the FN clones demonstrated that the constant domain of FN may be important in this interaction. The interaction was verified and characterized *in vitro* by surface plasmon resonance

(SPR) and immunoprecipitation experiments. To investigate the type IX collagen-FN interaction *in vivo*, we have analyzed bovine articular cartilage by immunohistochemistry showing that type IX collagen and FN co-localize within the cartilage matrix. These data provide evidence for an *in vivo* type IX collagen-FN interaction in articular cartilage.

EXPERIMENTAL PROCEDURES

Materials and Reagents—All reagents were obtained from Sigma unless otherwise stated. All yeast two-hybrid media and reagents were prepared according to the Matchmaker™ 3 manual (Clontech) and the yeast protocols handbook (Clontech) unless otherwise stated.

Plasmid Construction—A 750-bp sequence encoding the entire NC4 domain of human *COL9A1* (bases 10–753 of GenBank™ accession number NM_001851.2) was generated by a PCR of a human chondrocyte cDNA library (Clontech) with PCR primers (NC4F, 5′-tctgcagctgctaagcgtc-3′; NC4R, 5′-acctctctcgtcggtggtct-3′). Adapted NC4F and NC4R PCR primers containing NdeI and SalI restriction site linkers, respectively, were used to facilitate the cloning of the 750-bp NC4 sequence in-frame with the GAL4 DNA binding domain (DNA BD) in the bait plasmid, pGBKT7 (Clontech). The pGBKT7-NC4 construct was sequenced (ABI Prism 3100, PerkinElmer Life Sciences) to confirm the identity and the open reading frame (NCBI BLAST search engine (www.ncbi.nlm.nih.gov)).

Yeast Two-hybrid Library Screening—The Matchmaker™ 3 two-hybrid system was used to screen a human chondrocyte cDNA library (Clontech) for potential NC4 domain interacting partners. The cDNA library was generated by directional cloning of cDNAs generated from unstimulated or IL-1 or TGF-β-stimulated human primary chondrocytes into pACT2, retaining the reading frame with the GAL4 DNA transcriptional activation domain (AD). *Saccharomyces cerevisiae* strain, AH109 (*MATa, trp1-901, leu2-3, 112, ura3-52, his3-200, gal4Δ, gal80Δ, LYS::GAL1_{UAS}-GAL1_{TATA}-HIS3, GAL2_{UAS}-GAL2_{TATA}-ADE2, URA::MEL1_{UAS}-MEL1_{TATA}-lacZ*), was transformed with 0.5 μg of pGBKT7-NC4 plasmid using the polyethylene glycol/single strand DNA/lithium acetate transformation method (26), A large scale transformation of the DNA BD-NC4-transformed yeast cells that scaled up the standard high efficiency transformation protocol 90-fold was then used to screen 45 μg of amplified human chondrocyte AD-cDNA library. An interaction between the NC4 bait protein (fused to the DNA BD) and a library-encoded protein (fused to the AD) creates a novel transcription factor that activates the GAL4-responsive reporter genes, *ADE2*, *HIS3*, and *lacZ*. The transformed cells were spread onto 50 × 150 mm −Leu/−Trp/−His/−Ade plates and incubated for up to 14 days at 30 °C. Surviving colonies representing putative yeast two-hybrid positives were further screened for LacZ reporter expression using the β-galactosidase colony filter assay (27).

Plasmids were extracted from positive yeast cells as described previously (28) and transformed into *Escherichia coli* strain JM109 (29). Ampicillin (50 μg/ml) was used to select for transformants containing pACT2-cDNA plasmids, and kanamycin (100 μg/ml) was used to select for those containing pGBKT7-NC4 plasmids. Plasmids were purified from *E.coli*

using the Qiagen high speed midi kit according to the manufacturer's instructions.

Yeast Two-hybrid Interaction Verification—To confirm interactions, the cDNA library clones identified as interacting with the NC4 domain were co-transformed into yeast (AH109) with either the NC4 or control plasmids. The NC4-cDNA interaction was reconstructed in yeast by co-transformation of pGBKT7-NC4 and pACT2 cDNA. Control plasmids for the expression of proteins known to interact (pACT2-T antigen and pGBKT7-p53) were used to construct a positive control interaction. pACT2-cDNA transformed alone or co-transformed with either pGBKT7 alone or a pGBKT7-lamin C fusion was used as a negative control. All transformations were achieved using the polyethylene glycol/single strand DNA/lithium acetate transformation method (26), and each of the transformants was tested for reporter gene expression by growth on −Leu/−Trp/−His/−Ade agar plates and the β-galactosidase colony filter assay (27).

Analysis of Yeast Two-hybrid Interacting Clones—PCR primers designed to the flanking region of the pACT2 multiple cloning site (pACT2F 5′-gaacttgcggggtttttcagt-3′ and pACT2R 5′-cgcgtttggaatcactac-3′) were used to sequence several positive colonies where the interaction had been confirmed (ABI Prism 3100, PerkinElmer Life Sciences). Sequence data were analyzed using the NCBI BLAST search engine, NCBI ORF finder, DNAsis (Hitachi Software Engineering), Webcutter 2.0, and NCBI human genome data base (www.ncbi.nlm.nih.gov). Because a number of interacting clones encoded FN, PCR primers were designed to the C-terminal end of human FN (GenBank™ accession number X02761.1). FNF (5′-gtgggcaactctgtcaacgaa-3′) and FNR (5′-tcgggaatcttctctgtcacg-3′) primers were then used to PCR screen remaining interacting clones (pACT2-cDNA).

Immunoprecipitation of Fibronectin and α1(IX) NC4—To confirm the interaction between fibronectin and the α1(IX) NC4 domain, immunoprecipitation experiments were carried out using recombinant human NC4 (see below) and human fibronectin (Upstate).

Stable Transfection of HEK 293-EBNA Cell Line for Expression of Recombinant Human NC4 (rhNC4)—The human *COL9a1* NC4 sequence was amplified by PCR and inserted into the pCEP4 expression vector (Invitrogen) using KpnI and XhoI restriction sites. The reverse primer contained an engineered FLAG tag amino acid sequence on the C terminus of the NC4 domain followed by a stop codon and the XhoI restriction enzyme site (NC4r, CCC CCC TCG AGT CAC TTG TCA TCG TCG TCC TTG TAG TCT CTC TCG TCG GTG). An upstream forward primer encoded the first 20 nucleotides of the NC4 domain from the ATG start codon and included a KpnI restriction enzyme site (NC4f, CGG CGG TAC CCA TGA AGA CCT GCT GGA AAA TT). A pCEP4 vector containing the human NC4 sequence was prepared using the above restriction sites and standard cloning techniques (30). DNA preparations of the pCEP4 vector were sequenced to confirm the identity and orientation of the NC4 domain insert.

pCEP4 plasmid (2 μg) containing the NC4 domain was transfected into confluent human embryonic kidney (HEK) 293-EBNA (Invitrogen) cells using Lipofectin® (Invitrogen) according to the manufacturer's instructions. HEK 293-EBNA cells constitutively express the Epstein-Barr virus nuclear antigen-1 (EBNA-1) allowing for the high copy episomal replication of the *oriP* containing the pCEP4 vector. After 72 h cells were subcultured using standard protocols and transfected clones selected using hygromycin (300 μg/ml, Invitrogen) in complete DMEM containing 10% fetal calf serum (FCS). Clones expressing rhNC4 protein were expanded and maintained in the medium containing hygromycin.

To facilitate the purification and maintain production of rhNC4 secreted into the media, cells approaching confluency were cultured sequentially with complete DMEM containing 2% FCS and hygromycin and serum-free conditions using Ex-Cell® VPRO culture media containing hygromycin. The cell-conditioned serum-free media were removed for purification and replaced every 4 days.

Purification of rhNC4 by Affinity Column Chromatography—Serum-free media harvested from rhNC4 expressing HEK 295-EBNA cells was centrifuged at 10,000 × g for 15 min and filtered through a 0.2-μm filter. Protease inhibitors (100 μg/ml soybean trypsin inhibitor, 10 mM *N*-ethylmaleimide, 10 mM EDTA, and 1 mM phenylmethylsulfonyl fluoride) were added to the media, and 1 M Tris (pH 8.0) was added in a 1:10 ratio with media. An anti-FLAG affinity column was used to purify rhNC4 from the filtered serum-free culture media. A batch absorption method was used whereby 50 ml of filtered culture media were incubated with 1 ml of anti-FLAG resin for 1 h at 4 °C. The resin was washed with 15 ml of 0.15 M NaCl, 0.05 M Tris base (TBS) (pH 8.0), and the rhNC4 protein was eluted by competitive binding of a FLAG peptide at a concentration of 100 μg/ml in TBS. Between purifications, the column was stripped by washing the resin in 0.1 M glycine HCl (pH 3.5) followed by re-equilibration in TBS.

Immunoprecipitation—Purified rhNC4 was dialyzed against TBS (pH 8.0) at 4 °C for 16 h to remove any co-purifying FLAG peptide that may be present in the eluate, and the concentration of rhNC4 was determined by BCA protein analysis (Pierce). Protein complexes were allowed to form by incubating 2 μg of human fibronectin (hFN, Upstate) with 54 μg of the purified rhNC4 in TBS (pH 8.0) at 4 °C for 16 h. Protein complexes were precipitated using either anti-FLAG M2 monoclonal antibody (9.2 μg) or a rabbit polyclonal FN antibody raised against a recombinant protein corresponding to amino acids 2087–2386 at the C terminus of human FN (8 μg) (Santa Cruz Biotechnology) at room temperature for 1 h. In addition, to ensure specific antibody binding, rhNC4 (25 μg) alone was incubated with the anti-FN primary antibody (8 μg), and similarly hFN (1 μg) was incubated with the anti-FLAG primary antibody (9.2 μg) using identical conditions.

Antibody-bound protein complexes were recovered by interaction with protein G-Sepharose (GE Healthcare). Briefly, 50 μl of protein G-Sepharose was added to the antibody/protein mixtures and incubated at 4 °C for 1 h with gentle agitation, and Sepharose-bound immunoprecipitates were recovered by centrifugation at 12,000 × g for 20 s. The pellet was washed three times with TBS and resuspended in 30 μl of sample buffer (100 mM Tris-HCl, 2% SDS, 10% glycerol, 5% 2β-mercaptoethanol, 0.002% bromphenol blue). Samples were heated to 95 °C for 3

min and analyzed on polyacrylamide gels (10% (w/v)) in the presence of β-mercaptoethanol and Western blotting using nylon membranes (PVDF, Immobilon) (31, 32). Nonspecific sites on membranes were blocked by incubation in TBS (pH 8.0) containing 3% (w/v) skimmed milk powder for 30 min with shaking at room temperature. Membranes were then incubated with either anti-FLAG (1:2000) or anti-FN (1:500) in TBS (pH 8.0) containing 0.2% Tween 20, 1% (w/v) skimmed milk powder for 2 h at room temperature. Proteins were visualized using horseradish peroxidase-conjugated secondary antibodies (1:10,000), ECL reagent, and Hyperfilm (GE Healthcare) and compared with hFN and FLAG-tagged rhNC4 standards and molecular weight markers. Duplicate membranes were incubated without primary antibody to control for nonspecific secondary antibody binding.

Biomolecular Interaction Analysis—To confirm the interaction between type IX collagen and fibronectin, SPR was carried out using a BIAcore 3000. Whole type IX collagen (containing collagenous and noncollagenous domains) purified from rat chondrosarcoma (33) and pepsinized type IX collagen purified from bovine cartilage (33, 34) were solubilized in 10 mM sodium acetate (pH 4.0) and immobilized on individual flow cells on a CM5 chip (BIAcore). Immobilization levels were 500 resonance units (RU) for each ligand. As a control for changes in sample refractive index, a blank flow cell was subjected to the immobilization procedure without added protein. Human fibronectin (FN) (Upstate, 200 μg/ml) in running buffer (0.01 M HEPES (pH 7.4), 0.15 M NaCl, 0.005% surfactant P20) was injected over pepsinized and whole type IX collagen flow cells for 3 min at 30 μl/min with the uncoated surface as a reference. For affinity measurements, human cellular FN was injected in running buffer at 30 μl/min into the flow cells at concentrations 0–300 nM. The ligand surfaces were regenerated by two injections of 30 μl of 10 mM glycine (pH 2.0) between each experiment. No significant change in base-line readings was observed. The binding curves were obtained with reference to pepsinized type IX collagen.

To further verify this interaction, the ligand surfaces were reversed. Human cellular FN was immobilized to flow cells 2–4 on a CM5 chip using standard BIAcore protocols. Increasing levels of FN were immobilized to flow cells 2–4, whereby 2000 and 4000 RU were bound, respectively. Flow cell 1 was activated as a protein-negative surface acting as a control for changes in refractive index. Whole type IX collagen (60 μg/ml) was injected over FN flow cells with 2000 and 4000 RU for 3 min at 20 μl/min to demonstrate an increase in binding with increased FN on the chip surface. Pepsinized type IX collagen (100 μg/ml) was also injected over this FN-coated surface for 3 min at a flow rate of 10 μl/min to verify the specificity to the noncollagenous domains of type IX collagen in both SPR circumstances. For affinity kinetic analysis, a concentration series of whole type IX collagen (0–450 nM) diluted in running buffer was injected over the FN surface (flow cell 2) for 5 min at a flow rate of 20 μl/min. Regeneration of the ligand surfaces between each experiment was achieved by washing in 20 mM NaOH for 30 s at a flow rate of 30 μl/min. No significant change in base-line readings was observed. Binding curves were obtained with reference to the blank flow cell.

To determine affinity kinetics, sensogram data that was not required for analysis was removed ensuring that the association and dissociation binding events remained, followed by X and Y transformation of the curves. The association and dissociation rate constants were then determined using separate curve fits to the equation for 1:1 Langmuir binding in the BIAevaluation 3.1 software (BIAcore). The equilibrium dissociation constant (K_D) of the interaction was calculated from these values for each curve allowing a range of K_D values for this interaction to be determined.

Immunohistochemistry—Cryosections of articular cartilage, obtained from the carpal joints of 18-month-old cow, were immunofluorescently dual-labeled for fibronectin and type IX collagen. Full thickness articular cartilage was rapidly frozen in liquid nitrogen-cooled isopentane, and 20-μm sections (Bright's cryostat) were transferred to glass slides coated with VECTABOND^{TM} reagent (Vector Laboratories). Each step was performed at room temperature unless stated otherwise, and between each incubation step, sections were washed three times for 5 min in 0.01 M phosphate-buffered 0.13 M NaCl (PBS, pH 7.4) containing 0.001% Tween 20 (wash buffer). All antibodies were diluted in wash buffer.

Sections were circumscribed with a water-repellent pen (Dako), wet in wash buffer, and then digested in bovine testicular hyaluronidase (0.1 mg/ml) for 1 h at 37 °C. Sections were washed and blocked in goat serum (1:20 dilution; Dako) for 30 min prior to incubation with a rabbit polyclonal antibody to type IX collagen (anti-"M"; 1:25 (15)) for 2 h. Sections were washed and incubated with a goat anti-rabbit fluorescein isothiocyanate (FITC)-conjugated secondary antibody for 1 h (1:64), washed, and blocked as before prior to overnight incubation at 4 °C with an anti-human fibronectin monoclonal antibody (clone HFN36.3 10 μg/ml; Developmental Studies Hybridoma Bank, University of Iowa). Sections were washed, and a goat anti-mouse Alexa 594-conjugated secondary antibody (1:400 dilution; Invitrogen) was applied to the tissue sections for 1 h. Finally, sections were washed and mounted under coverslips with VECTASHIELD HardSet Mounting Medium with DAPI (Vector Laboratories). Immunofluorescent controls, which consisted of replacing the primary antibodies with "naïve" mouse and rabbit immunoglobulin (10 μg/ml; Dako) or buffer and switching the secondary antibodies, showed no nonspecific binding of primary or secondary antibodies (data not shown).

Sections were examined with a Leica TCS SP2 confocal microscope (Leica, Heidelberg, Germany) using a 63× oil immersion objective lens. To eliminate the possibility of spectral bleed through between fluorescent probes, representative regions were scanned using appropriate excitation and emission settings for sequential recordings of DAPI (excitation maximum of 358 nm; emission maximum of 461 nm), FITC (excitation maximum of 494 nm; emission maximum of 518 nm) and Alexa 594 (excitation maximum of 594 nm; emission maximum of 617 nm). Stacks of optical sections were sampled through the depth of the tissue section at a vertical spacing of 0.3– 0.5 μm. The frequency distributions of fluorescent intensities of green (collagen type IX) and red (fibronectin) fluorescent label in the resultant image stacks were then analyzed using Leica confocal
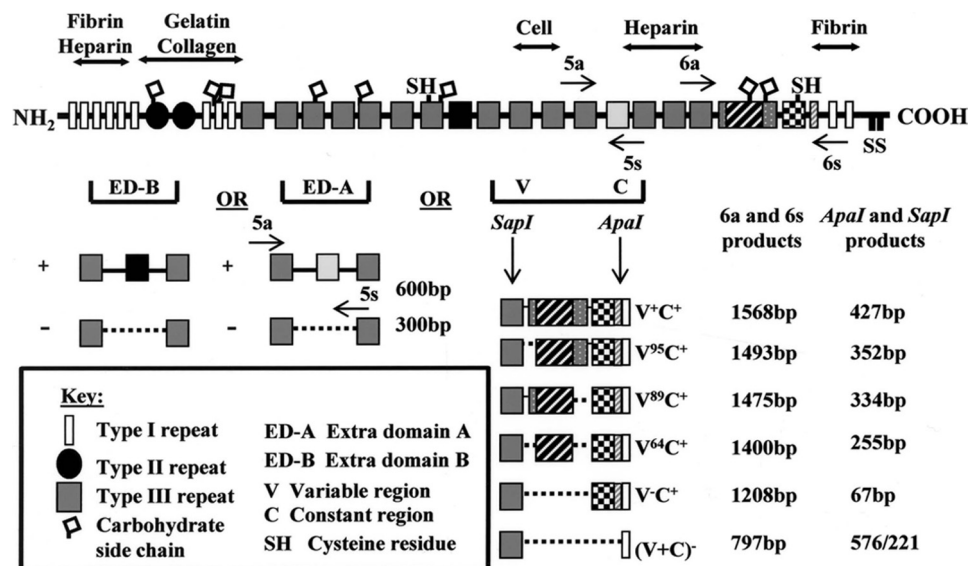
FIGURE 1. **Domain structure of human cellular FN showing previously characterized binding domains and possible isoforms because of alternative splicing.** Binding sites of primers that flank the ED-A domain (5a and 5s) and the variable region (6a and 6s) are shown (35). PCR product sizes for the 6a and 6s primer pair, 5a and 5s primer pair, and ApaI and SapI restriction digest products are indicated. *bp,* base pairs.
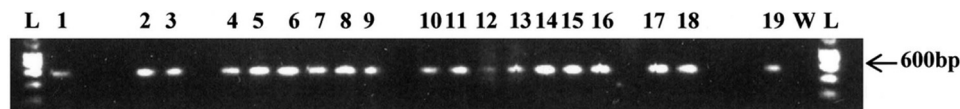

FIGURE 2. **PCR screen of the 26 isolated yeast two-hybrid positive clones with human FN primers indicates that the expected 588-bp amplimer is present in 19 of these positive clones, which are numbered as shown.** A 100-bp ladder (*L*; Promega) and water control (*W*) are shown.

software. The extent of co-localization was assessed in two ways: (i) from an analysis of scatter plots (cytofluorograms) of red/green pixel intensity distributions within the stack, thus allowing co-localized pixels to be highlighted within the image stack via a white binary overlay mask, and (ii) from a comparison of red/green pixel intensity profiles generated from line segments arbitrarily drawn upon red/green composite images within stacks.

Molecular Analysis of FN Variants—Previously published PCR primers (35) designed to the spliced ED-A (5a and 5s) and variable (6a and 6s) regions of FN were used to establish the splice variant identity of each of the FN isoforms encoded by the interacting clones (Fig. 1). Restriction digestion of 6a- and 6s-amplified PCR products with ApaI and SapI (New England Biolabs) was used to identify the presence of the alternatively spliced V region as it could not be clearly identified from 6a/6s product size (Fig. 1). 6a/6s PCR products were incubated with ApaI and SapI individually or both together (5 units of each) at 37 °C for 2.5 h. All the PCR and restriction digest products were visualized by ethidium bromide (1 μg/ml) staining of 1–2% agarose gels (30).

RESULTS

Yeast Two-hybrid Screening of a Human Chondrocyte cDNA Library—Screening 6.35×10^5 yeast chondrocyte library transformants identified 26 clones encoding proteins that potentially interacted with NC4 bait causing expression of all three reporter genes. DNA sequencing and PCR with human FN-specific primers identified 19 (73%) of these clones to encode human cellular FN (Fig. 2). The reconstruction of the interaction in yeast with all stated controls demonstrated that only the presence of both the NC4 domain and FN resulted in the expression of all three reporter genes (Fig. 3). These experiments also show that the identified interacting partner does not cause direct transcriptional activation of reporter genes and that it does not have affinity for the GAL4-DNA BD component of the hybrid protein or lamin-C.

Other positive clones identified in the yeast two-hybrid screen included tenascin C, splicing factor cc.1.3, attractin, and metallothionein. Such a high incidence of FN interacting clones (73%) dictated that this interaction be investigated further.

Fibronectin and NC4 Co-immunoprecipitation in Vitro—*In vitro* interaction between FN and NC4 was characterized further by co-immunoprecipitation (Fig. 4) using FLAG-tagged rhNC4 and hFN. rhNC4 and FN were mixed together and complexes immobilized onto anti-FLAG or anti-FN antibodies coupled to protein G-Sepharose. Western blot analysis using antibodies to either FN (Fig. 4*a*) or FLAG (Fig. 4*b*) confirmed that FN binds to NC4 *in vitro*. Bands were identified on the basis of relative mobility to known molecular weight, hFN and FLAG-tagged rhNC4 standards. In addition to a band detected for monomeric NC4 ($\Rightarrow$ NC4; Fig. 4*b*), further specific bands were observed which, from their molecular weight, were assumed to be NC4 dimers and multimers (*; Fig. 4*b*). Because the high molecular weight NC4 multimers appeared to co-migrate with FN, the α-FN blot was stripped and re-probed with the α-FLAG antibody (Fig. 4*c*). This confirmed that these bands were indeed multimers of NC4-FLAG and not FN as the α-FLAG antibody did not nonspecifically bind to FN (absence of band in FN standard lane; Fig. 4*c*).
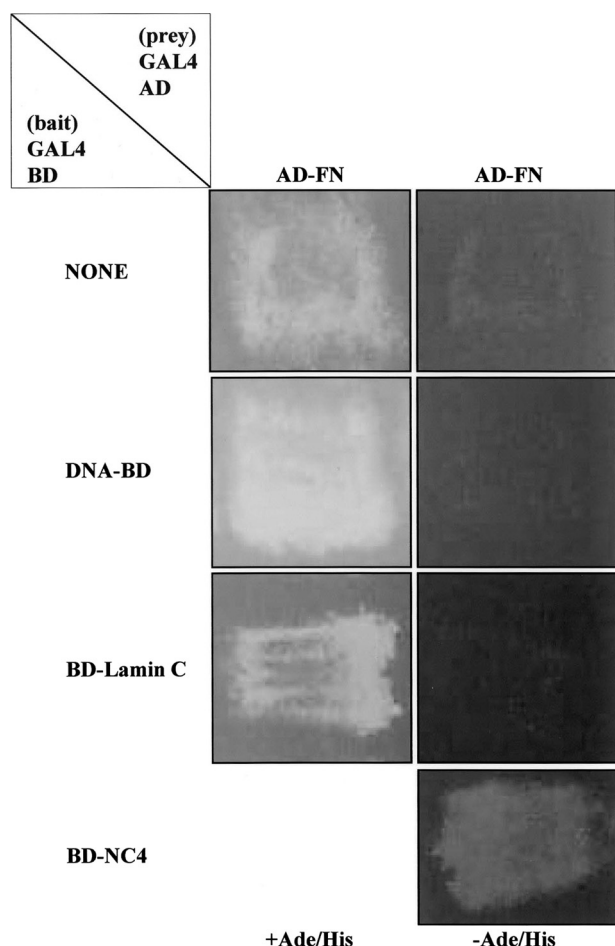
FIGURE 3. **NC4 domain of type IX collagen interacts with human cellular FN in the yeast two-hybrid system.** Yeast AH109 cells were co-transformed with the indicated GAL4 DNA BD bait and GAL4 AD prey plasmids. The lamin-C protein is not thought to interact with any other protein and therefore is an additional negative control plasmid. Yeast patches were grown on minimal media with (+*Ade/His*) or without (−*Ade/His*) adenine and histidine. Growth of yeast on −Ade/His is indicative of an interaction between bait and prey proteins. Only yeast containing the GAL4 DNA BD-NC4 plasmid and GAL4 AD-FN plasmid grew in the absence of Ade and His (*bottom panel*). These yeast cells were also the only cells that turned blue when all yeast transformants were replicated and analyzed for *lacZ* reporter gene activity (data not shown).

Duplicate membranes probed with secondary antibodies alone contained heavy and light IgG bands only and confirmed that the secondary antibodies did not nonspecifically bind to either NC4 or FN (Fig. 4, *d* and *e*). In addition, the specificity of antibody binding was confirmed indirectly by incubating rhNC4 (25 μg) alone with the anti-FN primary antibody (8 μg) and similarly incubated hFN (1 μg) with the anti-FLAG primary antibody (9.2 μg) using identical conditions (data not shown).

In Vitro Verification of the NC4-FN Interaction Using SPR— An interaction between whole type IX collagen and cellular FN was observed by SPR using the BIAcore 3000 system (Figs. 5 and 6). Binding of cellular FN to immobilized whole type IX collagen was observed, but no interaction was observed using pepsinized type IX collagen (data not shown). The latter was subsequently used as a reference in kinetic analysis experiments where type IX collagen was the ligand on the chip surface. Analysis of a concentration series of FN binding curves indicated that the interaction with NC4 has a 1:1 stoichiometry. Association and dissociation events were fitted to the 1:1 Langmuir model separately yielding a range of binding affinities (K_D) in the range of $1.31–5.28 \times 10^{-9}$ M (Fig. 5). The χ^2 values for the association and dissociation fits were 0.484 and 1.95, respectively.

When an increased amount of FN was immobilized to the chip surface (2000 or 4000 RUs) a corresponding increase in response signal was observed when whole type IX collagen was injected over it indicating that this interaction is specific (data not shown). The levels of FN ligand bound to the chip surface and therefore the signal responses observed are higher, but as a percentage of the R_{max}, both surfaces give binding events that represent ~13% of R_{max}. No binding response was observed when pepsinized type IX collagen was injected over this surface (data not shown). Whole type IX collagen concentration series analysis is consistent with the FN binding data, giving very similar binding affinities of 0.992×10^{-10} to 3.93×10^{-9} M (Fig. 6). The χ^2 values for the association and dissociation fits were 1.17 and 2.83, respectively.
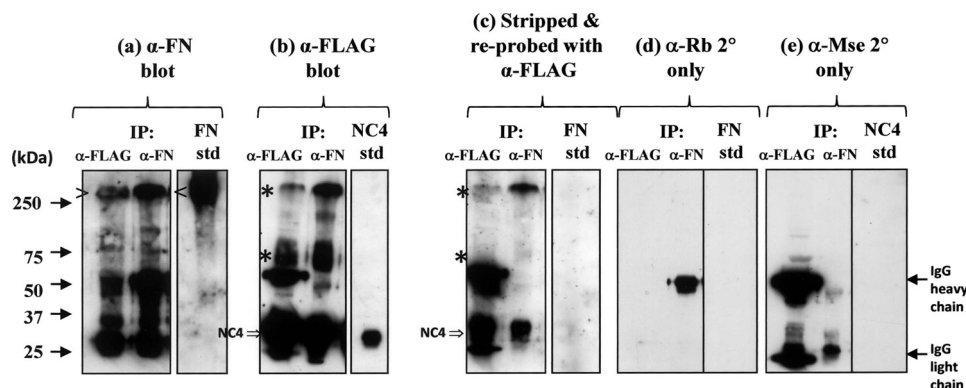

FIGURE 4. **Direct *in vitro* interaction of fibronectin and NC4.** FLAG-tagged rhNC4 and hFN were mixed together and immunoprecipitated with either anti-FLAG antibody (*IP: α-FLAG*) or anti-fibronectin antibody (*IP: α-FN*). The immunoprecipitated proteins were resolved on 10% (w/v) SDS-polyacrylamide gels and blotted with either anti-FN antibody (*a*) or anti-FLAG antibody (*b*). Bands were visualized by enhanced chemiluminescence and identified on the basis of relative mobility to known molecular mass (kDa) and hFN (*FN std*) and FLAG-tagged rhNC4 (*NC4 std*) standards. FN-positive bands are indicated (<). As well as a band detected for monomeric NC4 (⇒), additional specific bands were observed which, from their molecular weight, were identified to be NC4 dimers and multimers (*). To confirm specificity of the high molecular weight multimers, assumed to be NC4, anti-FN blots were stripped and reprobed with the anti-FLAG antibody (*c*). Finally, duplicate membranes were probed with secondary antibodies only to confirm the position of light and heavy IgG chains (→) and that there was no nonspecific cross-reactivity of the secondary antibodies with FN or NC4 (*d* and *e*).
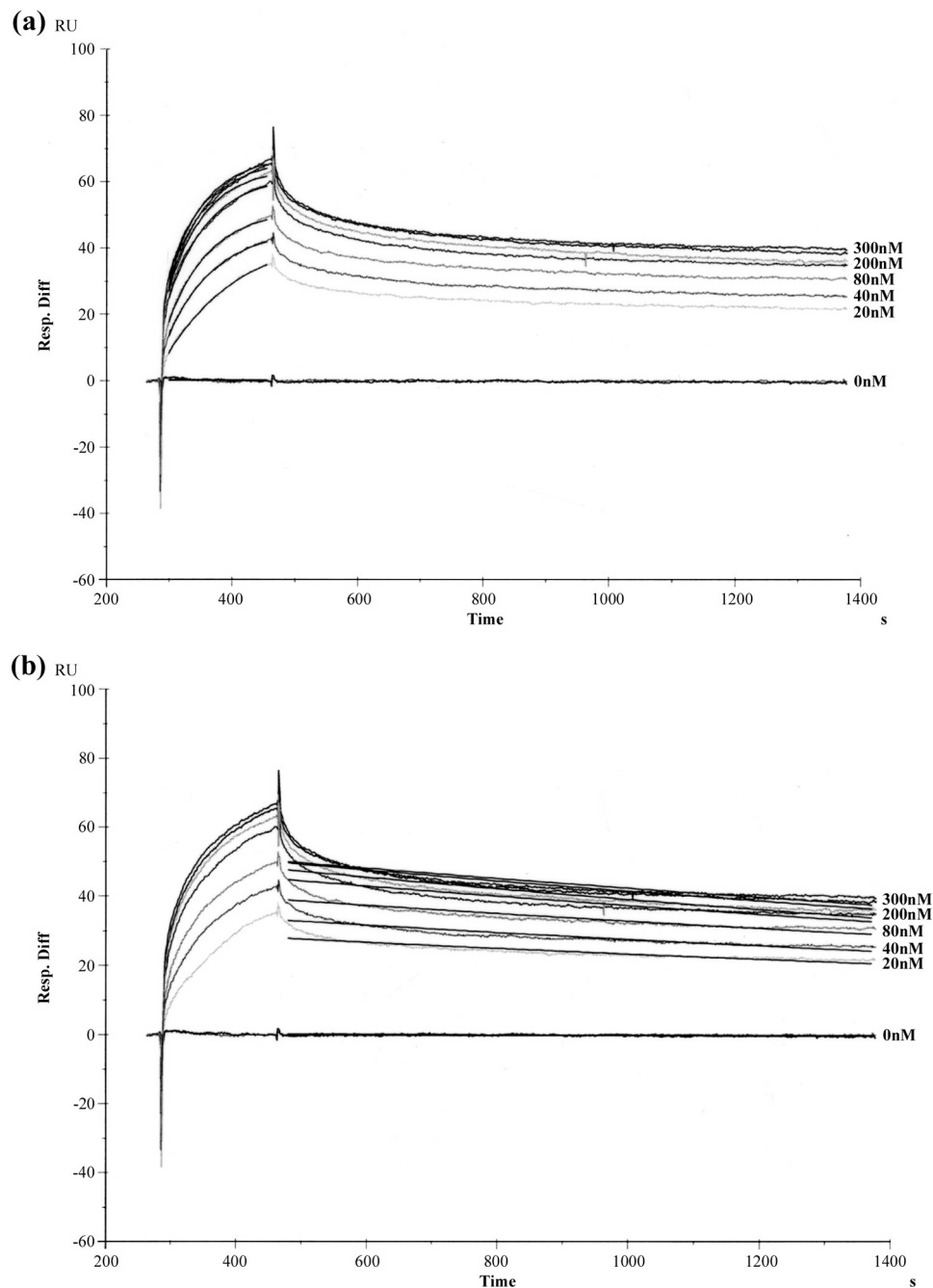
(a) RU

(b) RU

FIGURE 5. **SPR sensogram.** Analysis of a FN concentration series (0–300 nM) showing binding curves with curve fits for both association (*a*) and dissociation (*b*) events. 200 and 300 nM binding curves are in duplicate.

Type IX Collagen and FN Co-localize in Mature Bovine Articular Cartilage—Immunohistochemistry using dual labeling followed by three-dimensional reconstructions and two methods of image analysis established that FN and type IX collagen significantly co-localize in the pericellular matrix (Fig. 7). All control sections were negative (data not shown).

Analysis of Interacting Clones Encoding FN—The FN primary mRNA transcript is alternatively spliced to generate multiple FN isoforms (Fig. 1). In previous studies (36, 37), four sites have been described where alternative splicing of FN mRNA occurs; these are named extra domain-A (ED-A), extra domain-B (ED-B), the variable (V) region, and a constant region (C), which contains the III-15 and I-10 FN repeats (Fig. 1). In the human, the V region contains two 5′ splice donor sites and three 3′ splice acceptor sites resulting in a total of five splice variants generated from the V region alone (Fig. 1) (38).

Determination of the FN variant(s) that interact with NC4 was achieved by PCR screening of the 19 yeast two-hybrid interacting FN clones. Fig. 1 shows the product sizes expected following PCR using the ED-A primer pair, 5a and 5s, and the variable region primer pair, 6a and 6s. Also, following restriction digestion of the variable region PCR product using ApaI and SapI, product sizes were used to designate the different splice variants of human FN present in all of the FN clones.
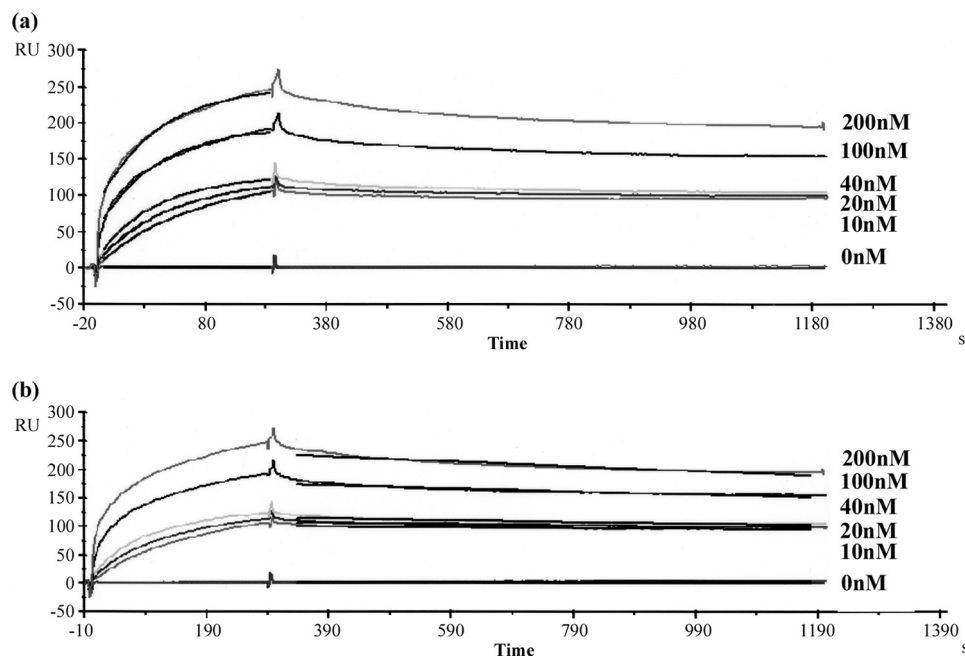
FIGURE 6. **SPR sensogram.** Analysis of a whole type IX collagen concentration series (0–200 nM) showing binding curves with curve fits for both association (*a*) and dissociation (*b*) events.

The ED-A domain was found to be present in 6 of the interacting FN clones (600-bp product) but absent from the remaining 13 (330-bp product) indicating that this domain is not required for an NC4-FN interaction to occur (Fig. 8*a*). PCR amplification with 6a and 6s revealed splicing out of the complete variable region (V^-C^+) in two of the interacting clones (4 and 19, 1208-bp product, Fig. 8*b*). All other FN clones produced PCR products >1400 bp indicating the inclusion of all or part of the variable region (Fig. 8*b*). The lack of a 797-bp PCR product in any of the interacting clones indicates that the cartilage-specific isoform, $(V+C)^-$, of FN was not identified as an NC4 binding partner (Fig. 8*b*), despite this isoform being present in the human cDNA chondrocyte library used for the yeast two-hybrid screen (data not shown).

The restriction digest of 6a and 6s generated PCR products with ApaI and SapI revealed that four different isoforms of the variable region (V^+C^+, $V^{95}C^+$, $V^{89}C^+$, and $V^{64}C^+$) were present in the 19 interacting FN clones (Fig. 8*c*). The presence of the V^-C^+ FN isoform was previously determined by PCR with 6a and 6s primers (Fig. 8*b*, *clones 4* and *19*).

DISCUSSION

The yeast two-hybrid assay enables the detection of protein-protein interactions within a eukaryotic expression system by utilizing the ability to functionally separate the DNA binding and activation domains of a detectable transcription factor (39). The screening of an adult human chondrocyte cDNA library with the NC4 domain of type IX collagen identified an interaction with the extracellular matrix glycoprotein, FN. The high incidence of interacting clones encoding FN (73%) suggests that this interaction is high affinity and may be important *in vivo*. The NC4-FN interaction was verified *in vitro* by immunoprecipitation using purified human proteins and NC4- and FN-specific antibodies.

Further analysis of the interaction was undertaken by SPR. Analysis of the interaction between FN and both native and pepsinized type IX collagen isolated from chondrosarcoma and cartilage, respectively, indicates a high affinity interaction with a 1:1 stoichiometry. Differential binding to whole and pepsinized type IX collagen demonstrated that one or more noncollagenous domains of type IX collagen are essential for the interaction. The commercially purified human FN, if contaminated with heparin, may have influenced the SPR as heparin has been shown to interact with the NC4 domain of type IX collagen (12). However, this appears unlikely because pepsinized type IX collagen also binds to heparin (40) and our data clearly indicate that the purified human FN preparation showed no affinity for pepsinized type IX collagen. This is consistent with the observed interaction being between FN and the noncollagenous domains of type IX collagen.

Sterically, the presentation of the NC4 domain on the surface of the cartilage collagen fibril (5, 6) renders it a more likely physiological ligand for FN within the native molecule than NC1, NC2, or NC3. The yeast two-hybrid, immunoprecipitation results, and the stoichiometry data strongly suggest that the 250 amino acid globular NC4 domain is the most likely candidate for the interaction observed by SPR. Furthermore, the high affinity of this interaction and its potential to occur periodically (7) along cartilage collagen fibrils strongly suggests that interaction of FN with NC4 at the surface of fibrils would result in a high valency interaction that consequently is important to the structural integrity of the cartilage matrix. This is supported by *in vivo* data demonstrating that overexpression of the NC4 domain of type IX collagen causes a degenerative joint disease phenotype in mice (21). As type IX collagen is involved in a number of interactions, it is only when subjected to mechanical stress, as demonstrated in the
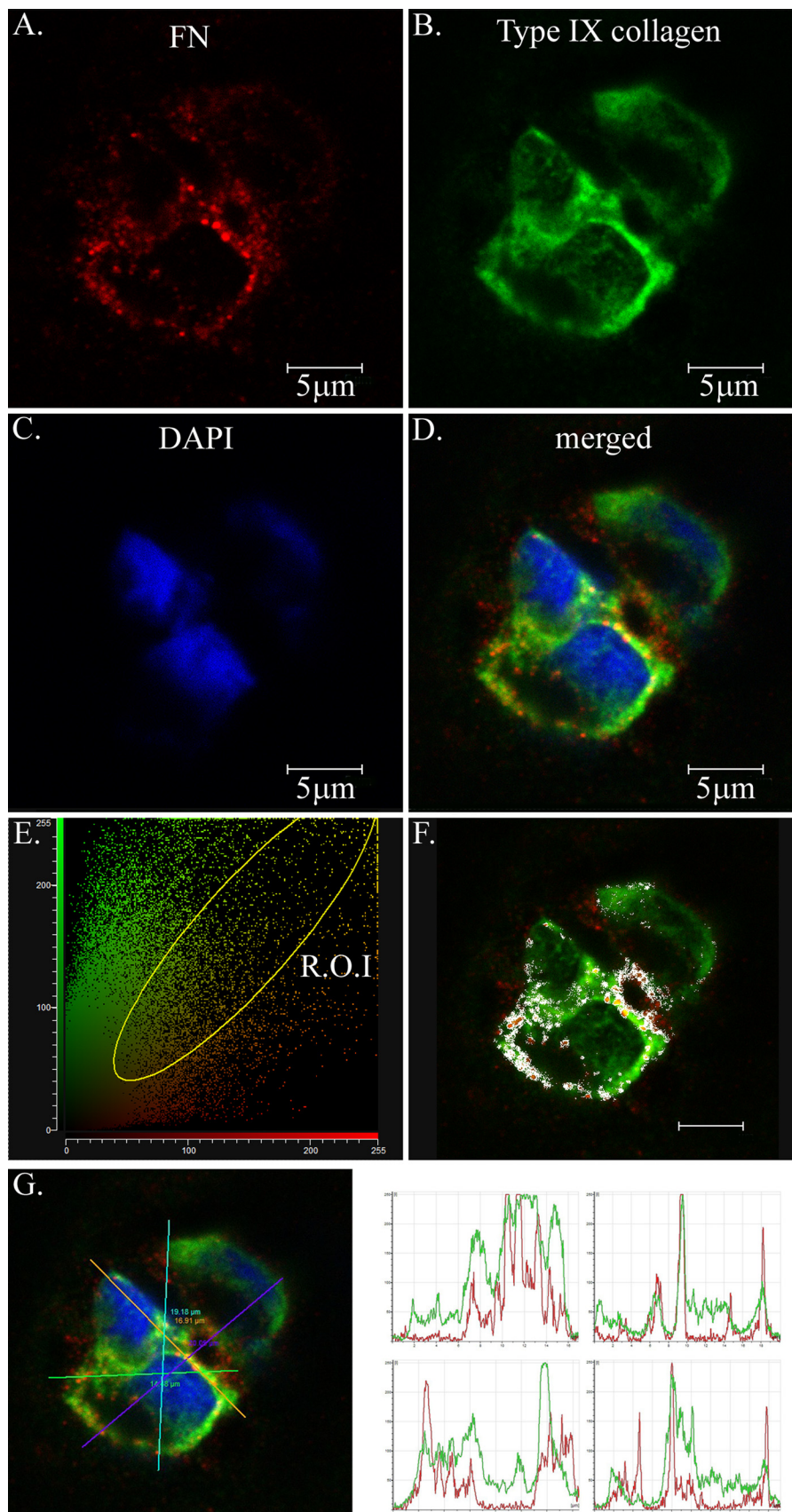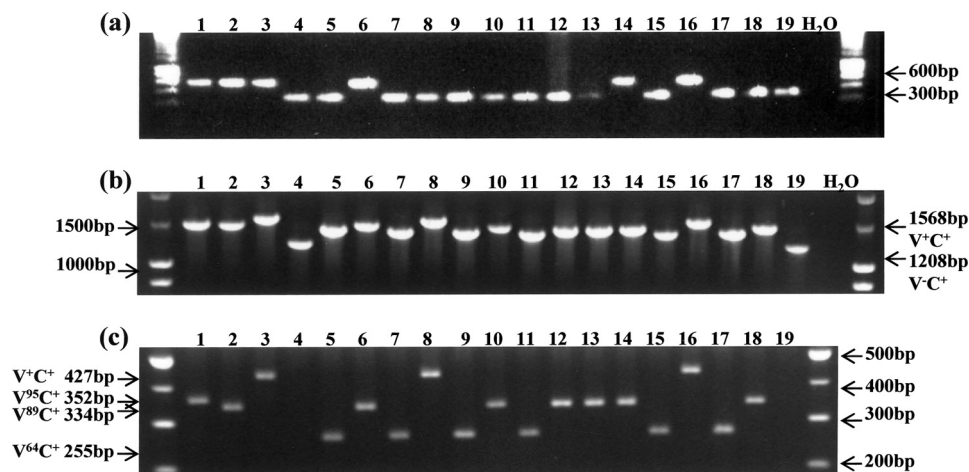
FIGURE 8. **FN splice variant analysis of interacting clones.** *a,* 1% agarose gel of PCR-amplified products using 5a and 5s primers showing the presence (600 bp) or absence (330 bp) of the ED-A domain in FN clones; *b,* 1% agarose gel of PCR-amplified variable region with 6a and 6s primers showing V^+C^+ variants (1568 bp: clones 3, 8, and 16) and V^-C^+ (1208 bp: clones 4 and 19) variants in FN clones; and *c,* 2% agarose gel of restriction digest products of FN clones using ApaI and SapI to determine the variable region isoform identity of each clone. Each of the different FN isoforms are indicated with their respective sizes.

Col9 and TSP5 double knock-out (23), that joint degeneration becomes apparent.

FN has been established as part of the repertoire of matrix molecules produced by the chondrocytes to assemble a functional and unique cartilage matrix (36). FN forms a distinct fibrillar network within the ECM, providing an environment essential for specific cell and tissue functions (41) and participating in cell adhesion, migration, proliferation, and differentiation (for review see Ref. 38). FN is composed of a series of homologous domains, termed type I, II, and III repeats (Fig. 1), which form an extended flexible molecule extremely sensitive to proteolytic digestion. The cell binding domain of FN contains an RGD sequence in the III-10 repeat that is essential for binding to cells via several integrins, including the FN-specific integrin $\alpha5\beta1$, which is the predominant integrin on the surface of articular cartilage chondrocytes (42, 43). FN also possesses heparin binding domains that interact with cell surface syndecans (44, 45). These interactions suggest that FN attachment could be important in cartilage homeostasis.

Numerous alternatively spliced isoforms of human FN have been reported (Fig. 1) (46). In this study, analysis of the FN splice patterns within the interacting clones has enabled the identification of regions of importance. The FN clones that were found to interact with the NC4 domain contained splice forms with and without the ED-A domain, indicating that the presence of this domain is not critical for this interaction to occur. In the developing chick, mesenchymal cells produce ED-B$^+$/ED-A$^+$ FN mRNA, but after differentiation the splicing pattern is switched to ED-B$^+$/ED-A$^-$ in embryonic chondrocytes (47). Analysis of ED-A domain expression levels in adult articular cartilage has shown that only 2–4% of FN is represented by this isoform in canine and human tissue (48–50) indicating this domain is unlikely to contribute significantly to mature cartilage ECM homeostasis. As only some of our interacting clones contained the ED-A domain, this domain is not essential for the interaction with the NC4 domain of type IX collagen *in vivo*. Identification of the ED-A-containing isoform within the human adult chondrocyte cDNA library suggests that the pretreatment with either IL-1 and/or TGF-β resulted in up-regulation of this isoform and may be worthy of further investigation.

Isoform representation of the variable region within each interacting clone is also not consistent, suggesting this region is not essential for the NC4-FN interaction, especially because in two of the interacting clones the V region is completely absent (V^-C^+ isoform). Expression of the cartilage-specific form $(V+C)^-$, which has been found in dog, horse, and rabbit adult articular cartilage at the mRNA level but absent in 11 other equine tissues screened (35), would be of particular interest. However, the cartilage-specific variant, $(V+C)^-$, was not detected in our yeast two-hybrid screen even though analysis of the human chondrocyte cDNA library confirmed that the $(V+C)^-$ FN isoform is represented, accounting for at least 10% of the FN clones.

On analysis of the clones that were positive for the NC4-FN interaction, the constant region was found to be universally present, indicating the importance of this region in the interaction. The fact that the $(V+C)^-$ isoform is present in the cDNA library but was not identified as interacting with the NC4

FIGURE 7. **Type IX collagen and FN co-localize in bovine articular cartilage.** Cryosections of articular cartilage, obtained from the carpal joints of 18-month-old cows, were immunofluorescently dual-labeled for FN (Alexa 594, *red*) and type IX collagen (FITC, *green*), and nuclei counterstained with DAPI (*blue*). Representative regions were scanned using appropriate excitation and emission settings for sequential recordings of Alexa 594 (*A*), FITC (*B*), and DAPI (*C*). The merged image of all three colors in *A–C* is shown in *D*. Stacks of optical sections were sampled through the depth of the tissue section at a vertical spacing of 0.3–0.5 μm. The frequency distributions of fluorescent intensities of *green* (collagen type IX) and *red* (fibronectin) fluorescent label in the resultant image stacks were then analyzed using Leica confocal software. The extent of co-localization was assessed by an analysis of scatter plots (cytofluorograms) of *red/green* pixel intensity distributions within the stack. This allowed co-localized pixels to be identified within a region of interest (*ROI*) (shown by *yellow diagonal ellipse*); *E,* co-localized pixels, identified within the *yellow ellipse* in *E,* are highlighted within the image stack via a *white* binary overlay mask (*F*). In addition, co-localization can be seen by comparison of *red/green* pixel intensity profiles generated from line segments arbitrarily drawn upon *red/green* composite images within stacks (*G*). *Bar,* 5 μm.

domain substantiates the finding that the constant region of FN is required for this interaction.

As discussed earlier, to be considered of relevance to cartilage function and integrity, the presence and proximity of interacting molecules have to be ascertained. With age, cartilage composition changes and chondrocyte density decreases, resulting in a reduction in cartilage metabolism and an inability to repair effectively. In normal adult cartilage, the rate of turnover of the fibrillar type II collagen component is limited (51), and collagen types VI, IX, and XI become more restricted to the pericellular matrix with increasing age (16) with a loss of the NC4 domain of the type IX collagen from the inter-territorial matrix (18). Although type IX is concentrated pericellularly in skeletally mature cartilage, a more uniform distribution is observed in fetal tissue (1). FN expression also changes with age, and mRNA expression of the noninteracting $(V+C)^-$ FN isoform has been shown to be increased after maturation in canine articular cartilage (52). Together, these data suggest that the FN-NC4 interaction that we have identified may be required during the high levels of cartilage matrix remodeling that accompany growth and repair, providing optimal stabilization and organization of the cartilage matrix. With maturation and decreased cartilage matrix turnover, it is possible that the NC4-FN interaction is only required and therefore maintained in regions of high turnover such as the pericellular environment.

Elucidation of the interactions within cartilage is fundamental to understanding the loss of cartilage integrity observed in disease. Both FN and FN proteolytic fragments are increased in human OA and rheumatoid arthritis suggesting an involvement in joint pathology (53). These FN fragments induce a catabolic response that results in a severe loss of cartilage proteoglycan, an early characteristic of OA, both *in vitro* and *in vivo* (54, 55). However, at much lower concentrations, FN fragments have an anabolic effect on cartilage metabolism, such as promoting an increased release of TGF-β and insulin-like growth factor-1 (56, 57). Therefore, FN and FN fragments are implicated as important regulators of normal cartilage homeostasis and cartilage degeneration during disease progression.

Our immunolocalization studies confirm previously described type IX collagen and FN distribution in normal articular cartilage (58, 59) and provide strong evidence of their co-localization within the pericellular matrix. The pericellular localization for both of these extracellular matrix proteins is characteristic of that observed in several species, and both increased age and disease enhance the predominance of specific antibody binding to the pericellular environment (16, 59). Thus, the co-localization of FN and type IX collagen is consistent with an *in vivo* interaction in cartilage. In addition to the areas around each cell where FN and type IX collagen interact, there are also areas where they exist independently. We speculate that this is due to a dynamic interaction that may, in part, be regulated by mechanical influences. Demonstration of such is beyond the scope of this study. The predominantly pericellular localization of both type IX collagen and FN suggests that there may be direct or indirect interaction with the chondrocyte itself, and a chondroprotective role for type IX collagen has previously been postulated (60). This has led to our hypothesis that type IX collagen is a molecular bridge between matrix components and the chondrocyte. Further studies are required to determine whether chondrocytes bind to the type IX-FN complex and whether this is mediated through the $\alpha5\beta1$ integrin and/or syndecans. The FN-specific, $\alpha5\beta1$ integrin is a mechanosensor in chondrocytes (43, 61) and may provide an extracellular signaling pathway that can transmit mechanical stimuli from the matrix to the cell. Loss of this NC4-FN interaction may compromise the ability of the chondrocyte to respond to mechanical signals and therefore predispose the cartilage matrix to OA-like degradation.

In summary, we have identified and confirmed a novel high affinity interaction between the NC4 domain of type IX collagen and FN using the yeast two-hybrid system, immunoprecipitation and SPR analysis. Immunohistochemistry has shown that type IX collagen and FN co-localize in close enough proximity in the ECM for this interaction to occur *in vivo*. Molecular analysis of the NC4-FN interacting clones established that both the ED-A domain and the variable region are not responsible for the interaction, and we have identified the constant region of FN as a strong candidate for the binding site. This study has provided evidence that this interaction likely exists in articular cartilage and could therefore contribute to the matrix integrity of the tissue.

REFERENCES

1. Eyre, D. R., Pietka, T., Weis, M. A., and Wu, J. J. (2004) *J. Biol. Chem.* **279,** 2568–2574
2. Fernandes, R. J., Schmid, T. M., and Eyre, D. R. (2003) *Eur. J. Biochem.* **270,** 3243–3250
3. Mendler, M., Eich-Bender, S. G., Vaughan, L., Winterhalter, K. H., and Bruckner, P. (1989) *J. Cell Biol.* **108,** 191–197
4. Wu, J. J., Woods, P. E., and Eyre, D. R. (1992) *J. Biol. Chem.* **267,** 23007–23014
5. Olsen, B. R. (1997) *Int. J. Biochem. Cell Biol.* **29,** 555–558
6. Duance, V. C., Vaughan-Thomas, A., Wardale, R. J., and Wotton, S. F. (1999) in *Biology of the Synovial Joint* (Archer, C. W., Caterson, B., Benjamin, M., and Ralphs, J. R., eds) pp. 135–163, Harwood Academic Publishers, Amsterdam
7. Vaughan, L., Mendler, M., Huber, S., Bruckner, P., Winterhalter, K. H., Irwin, M. I., and Mayne, R. (1988) *J. Cell Biol.* **106,** 991–997
8. Käpylä, J., Jäälinoja, J., Tulla, M., Ylöstalo, J., Nissinen, L., Viitasalo, T., Vehviläinen, P., Marjomäki, V., Nykvist, P., Säämänen, A. M., Farndale, R. W., Birk, D. E., Ala-Kokko, L., and Heino, J. (2004) *J. Biol. Chem.* **279,** 51677–51687
9. Holden, P., Meadows, R. S., Chapman, K. L., Grant, M. E., Kadler, K. E., and Briggs, M. D. (2001) *J. Biol. Chem.* **276,** 6046–6055
10. Mann, H. H., Ozbek, S., Engel, J., Paulsson, M., and Wagener, R. (2004) *J. Biol. Chem.* **279,** 25294–25298
11. Budde, B., Blumbach, K., Ylöstalo, J., Zaucke, F., Ehlen, H. W., Wagener, R., Ala-Kokko, L., Paulsson, M., Bruckner, P., and Grässel, S. (2005) *Mol. Cell. Biol.* **25,** 10465–10478

12. Pihlajamaa, T., Lankinen, H., Ylöstalo, J., Valmu, L., Jäälinoja, J., Zaucke, F., Spitznagel, L., Gösling, S., Puustinen, A., Mörgelin, M., Peränen, J., Maurer, P., Ala-Kokko, L., and Kilpeläïnen, I. (2004) *J. Biol. Chem.* **279,** 24265–24273

13. Tillgren, V., Onnerfjord, P., Haglund, L., and Heinegård, D. (2009) *J. Biol. Chem.* **284,** 28543–28553

14. Nishimura, I., Muragaki, Y., and Olsen, B. R. (1989) *J. Biol. Chem.* **264,** 20033–20041

15. Duance, V. C., Shimokomaki, M., and Bailey, A. J. (1982) *Biosci. Rep.* **2,** 223–227

16. Duance, V. C., and Wotton, S. F. (1991) *Biochem. Soc. Trans.* **19,** 376S

17. Wotton, S. F., Jeacocke, R. E., Maciewicz, R. A., Wardale, R. J., and Duance, V. C. (1991) *Histochem. J.* **23,** 328–335

18. Vaughan-Thomas, A., Dudhia, J., Bayliss, M. T., Kadler, K. E., and Duance, V. C. (2008) *Connect. Tissue Res.* **49,** 374–382

19. Nakata, K., Ono, K., Miyazaki, J., Olsen, B. R., Muragaki, Y., Adachi, E., Yamamura, K., and Kimura, T. (1993) *Proc. Natl. Acad. Sci. U.S.A.* **90,** 2870–2874

20. Fässler, R., Schnegelsberg, P. N., Dausman, J., Shinya, T., Muragaki, Y., McCarthy, M. T., Olsen, B. R., and Jaenisch, R. (1994) *Proc. Natl. Acad. Sci. U.S.A.* **91,** 5070–5074

21. Haimes, H. B., Jimenez, P. A., Li, Y., Shinya, T., and Olsen, B. R. (1995) *Inflamm. Res.* **44,** Suppl. 2, 127–128

22. Blumbach, K., Bastiaansen-Jenniskens, Y. M., DeGroot, J., Paulsson, M., van Osch, G. J., and Zaucke, F. (2009) *Arthritis Rheum.* **60,** 3676–3685

23. Posey, K. L., Hankenson, K., Veerisetty, A. C., Bornstein, P., Lawler, J., and Hecht, J. T. (2008) *Am. J. Pathol.* **172,** 1664–1674

24. Briggs, M. D., and Chapman, K. L. (2002) *Hum. Mutat.* **19,** 465–478

25. Czarny-Ratajczak, M., Lohiniva, J., Rogala, P., Kozlowski, K., Perälä, M., Carter, L., Spector, T. D., Kolodziej, L., Seppänen, U., Glazar, R., Królewski, J., Latos-Bielenska, A., and Ala-Kokko, L. (2001) *Am. J. Hum. Genet.* **69,** 969–980

26. Gietz, R. D., Schiestl, R. H., Willems, A. R., and Woods, R. A. (1995) *Yeast* **11,** 355–360

27. Gietz, R. D. (2006) *Methods Mol. Biol.* **313,** 345–371

28. Hoffman, C. S., and Winston, F. (1987) *Gene* **57,** 267–272

29. Hanahan, D. (1983) *J. Mol. Biol.* **166,** 557–580

30. Sambrook, J., Fritsch, E. F., and Manniatis, T. (1989) *Molecular Cloning: A Laboratory Manual*, 2nd Ed., Cold Spring Harbor Laboratory Press, Cold Spring Harbor, NY

31. Laemmli, U. K. (1970) *Nature* **227,** 680–685

32. Towbin, H., Staehelin, T., and Gordon, J. (1979) *Proc. Natl. Acad. Sci. U.S.A.* **76,** 4350–4354

33. Duance, V. C., Wotton, S. F., Voyle, C. A., and Bailey, A. J. (1984) *Biochem. J.* **221,** 885–889

34. Shimokomaki, M., Duance, V. C., and Bailey, A. J. (1980) *FEBS Lett.* **121,** 51–54

35. MacLeod, J. N., Burton-Wurster, N., Gu, D. N., and Lust, G. (1996) *J. Biol. Chem.* **271,** 18954–18960

36. Burton-Wurster, N., Lust, G., and Macleod, J. N. (1997) *Matrix Biol.* **15,** 441–454

37. Schwarzbauer, J. E. (1991) *Curr. Opin. Cell Biol.* **3,** 786–791

38. Hynes, R. O. (1990) in *Fibronectins* (Rich, A., ed) pp. 1–538, Springer-Verlag, New York

39. Fields, S., and Song, O. (1989) *Nature* **340,** 245–246

40. Munakata, H., Takagaki, K., Majima, M., and Endo, M. (1999) *Glycobiology* **9,** 1023–1027

41. Schwarzbauer, J. E., and Sechler, J. L. (1999) *Curr. Opin. Cell Biol.* **11,** 622–627

42. Loeser, R. F., Carlson, C. S., and McGee, M. P. (1995) *Exp. Cell Res.* **217,** 248–257

43. Salter, D. M., Hughes, D. E., Simpson, R., and Gardner, D. L. (1992) *Br. J. Rheumatol.* **31,** 231–234

44. Elenius, K., Salmivirta, M., Inki, P., Mali, M., and Jalkanen, M. (1990) *J. Biol. Chem.* **265,** 17837–17843

45. Saunders, S., and Bernfield, M. (1988) *J. Cell Biol.* **106,** 423–430

46. Kornblihtt, A. R., Pesce, C. G., Alonso, C. R., Cramer, P., Srebrow, A., Werbajh, S., and Muro, A. F. (1996) *FASEB J.* **10,** 248–257

47. Bennett, V. D., Pallante, K. M., and Adams, S. L. (1991) *J. Biol. Chem.* **266,** 5918–5924

48. Burton-Wurster, N., Leipold, H. R., and Lust, G. (1988) *Biochem. Biophys. Res. Commun.* **154,** 1088–1093

49. Rencic, A., Gehris, A. L., Lewis, S. D., Hume, E. L., and Bennett, V. D. (1995) *Osteoarthritis Cartilage* **3,** 187–196

50. Zhang, D. W., Burton-Wurster, N., and Lust, G. (1995) *J. Biol. Chem.* **270,** 1817–1822

51. Bank, R. A., Bayliss, M. T., Lafeber, F. P., Maroudas, A., and Tekoppele, J. M. (1998) *Biochem. J.* **330,** 345–351

52. Burton-Wurster, N., Borden, C., Lust, G., and Macleod, J. N. (1998) *Matrix Biol.* **17,** 193–203

53. Homandberg, G. A. (1999) *Front. Biosci.* **4,** 713–730

54. Homandberg, G. A., Meyers, R., and Xie, D. L. (1992) *J. Biol. Chem.* **267,** 3597–3604

55. Homandberg, G. A., Meyers, R., and Williams, J. M. (1993) *J. Rheumatol.* **20,** 1378–1382

56. Homandberg, G. A., and Hui, F. (1994) *Arch. Biochem. Biophys.* **311,** 213–218

57. Homandberg, G. A., Hui, F., Wen, C., Purple, C., Bewsey, K., Koepp, H., Huch, K., and Harris, A. (1997) *Biochem. J.* **321,** 751–757

58. Duance, V. C., Wotton, S. F., and Young, R. D. (1990) *Ann. N.Y. Acad. Sci.* **580,** 480–483

59. Pfander, D., Rahmanzadeh, R., and Scheller, E. E. (1999) *J. Rheumatol.* **26,** 386–394

60. Poole, C. A., Wotton, S. F., and Duance, V. C. (1988) *Histochem. J.* **20,** 567–574

61. Wright, M. O., Nishida, K., Bavington, C., Godolphin, J. L., Dunne, E., Walmsley, S., Jobanputra, P., Nuki, G., and Salter, D. M. (1997) *J. Orthop. Res.* **15,** 742–747